

# Resonant photoemission spectroscopy of thick Mn films on Si(111) at the $2p$ edge: Detection of the two-hole valence-band satellite of Mn

Marco Zangrando, Elena Magnano, and Alessandro Nicolaou

*Laboratorio Nazionale TASC INFN-CNR, S.S. 14 Km 163.5 in Area Science Park, 34012 Trieste, Italy*

Emanuela Carleschi

*Dipartimento di Fisica, Università di Trieste, via Valerio 2, 34127 Trieste, Italy*

Fulvio Parmigiani

*Dipartimento di Fisica, Università di Trieste, via Valerio 2, 34127 Trieste, Italy*

*and Laboratorio Nazionale TASC INFN-CNR, S.S. 14 Km 163.5 in Area Science Park, 34012 Trieste, Italy*

(Received 28 June 2006; revised manuscript received 28 November 2006; published 7 June 2007)

We have measured valence-band spectra of a thick Mn metal film deposited on Si(111) by means of resonant photoemission across the Mn  $2p \rightarrow 3d$  absorption edge. A resonant Raman-Auger signal is detected for excitation energies down to 3.8 eV below the Mn  $L_3$  absorption threshold. This feature exhibits a crossover from the Raman to the normal Auger behavior at a photon energy close to the Mn  $2p$  photoemission ionization threshold. The resulting radiationless resonance Raman behavior gives rise to a signal equivalent to the 6 eV satellite in Ni, with energy at 3.3 eV below  $E_F$ . Moreover, the presence of many-electron effects is detected for the Mn spectral weight in the valence band, with a clear contribution of Mn-derived states at the Fermi edge.

DOI: [10.1103/PhysRevB.75.233402](https://doi.org/10.1103/PhysRevB.75.233402)

PACS number(s): 78.66.Bz, 73.20.At, 79.60.Dp, 78.70.Dm

## INTRODUCTION

Mn can be considered as the most complex of all metallic elements, adopting four different modifications as a function of temperature. For  $\alpha$ -Mn (below 1000 K),<sup>1</sup> a clear understanding of the electronic structure is still lacking due to the complexity of its crystal structure, which still presents unresolved structural issues.<sup>2</sup> Moreover, only few valence-band photoemission data are reported in literature.<sup>3,4</sup>

Resonant photoemission spectroscopy (RPES) of the valence band (VB) has been shown to be a powerful tool to study electronic structure.<sup>5,6</sup> The loss of coherence going from the Raman to the normal Auger regime is caused by the delocalization of the photoexcited electron in the intermediate state.<sup>7</sup> Moreover, in order to observe Raman behavior, the localization time of the intermediate state ( $3d$  photoexcited electron) should be comparable to the  $2p$  core-hole autoionization time.<sup>8</sup> The crossover between the Raman and the normal Auger regimes is related to the ionization threshold (IT) measured as the binding energy (BE) of the  $2p_{3/2}$  level, which is the smallest energy needed to excite a core-level electron to the VB.<sup>9</sup>

In the case of  $3d$  transition metals (TMs), Raman behavior has been observed below the  $L_3$  absorption threshold in Ti,<sup>10</sup> V,<sup>9</sup> Cr, and Fe.<sup>11</sup> In all these cases, the IT energy is smaller than the absorption maximum (resonance) energy. For Ni metal, IT coincides with the resonance energy,<sup>11</sup> and the crossover is located exactly at this energy.<sup>12</sup> As a consequence, the conclusion drawn from measurements at the  $3p$  resonances that  $3d$  TMs with atomic number lower than Ni do not show two-hole satellites in the VB (Ref. 6) has been reformulated.<sup>11</sup> It has been shown that radiationless resonance Raman spectroscopy (RRAS) is a possible tool to investigate and detect these structures.<sup>12</sup>

To our knowledge, Mn metal has never been studied by RPES at the  $2p \rightarrow 3d$  edge, leaving the transition-metal series

from V to Ni incomplete. Raaen and Murgai using the  $3p \rightarrow 3d$  edge predicted the absence of satellites in the VB.<sup>13</sup> For Mn compounds, on the other hand, several RPES experiments have been performed tuning the photon energy across the  $L_3$  absorption threshold.<sup>7,8,14,15</sup>

In this paper, we present a room-temperature study of Mn metal thick films using resonant photoemission and, in particular, the RRAS technique to detect and characterize the two-hole satellite of Mn in the VB. In addition, we tune the incoming photon energy across the  $L_3$  absorption threshold in order to track the transition from the resonant Raman-Auger regime (constant BE) to the normal Auger regime [constant kinetic energy (KE)]. Finally, we identify the spectral weight of the Mn state in the VB region.

## EXPERIMENT

The experiments were performed at the BACH beamline of ELETTRA (Trieste), measuring (resonant) photoemission spectroscopy (PES) and x-ray-absorption spectroscopy (XAS) spectra.<sup>16</sup> RPES and XAS measurements have been taken in circular polarization at a grazing angle of  $10^\circ$ . The beamline was operated between 630 and 660 eV at an energy resolution of about 0.25 eV with a photon flux of  $\sim 2 \times 10^{11}$  photons/s on the sample. Both PES and XAS measurements were acquired in ultrahigh vacuum at a base pressure of  $2 \times 10^{-10}$  mbar. PES spectra were collected using an angle-integrated electron analyzer used, in the present case, with a relaxed resolution of about 200 meV. XAS spectra were acquired in partial electron yield mode. The total energy resolution was kept at about 0.33 eV during RPES.

The Si(111) surface was prepared by cycles of annealing at 1200 °C, keeping the pressure lower than  $1 \times 10^{-9}$  mbar. The contamination was checked by means of PES on the O 1s, C 1s, and Si  $2p$  core levels. A thick Mn layer ( $\sim 10$

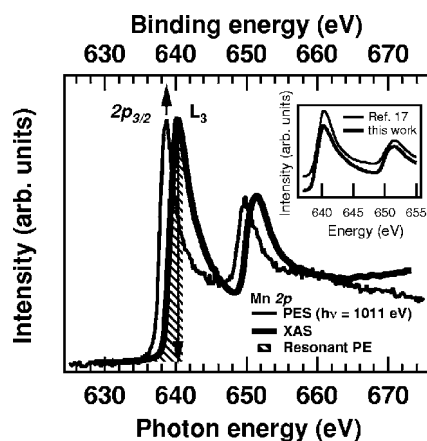


FIG. 1. Mn  $2p$  PES (thin line) and XAS spectra (thick line). The upper scale represents the BE for the PES and the lower scale the photon energy for the absorption. The description of the features and of the inset is in the text.

ML) was evaporated on the clean Si using an electron-beam evaporator operating at a constant rate of  $\sim 0.1$  Å/min.

## RESULTS AND DISCUSSION

In Fig. 1, we report the Mn  $2p$  PE spectrum measured with a photon energy ( $h\nu$ ) of 1011 eV and the Mn  $2p$  XAS spectrum. The positions of the Mn  $2p_{3/2}$  and  $2p_{1/2}$  PES maxima (ionization thresholds) are found to be 638.7 (EB) and 649.7 eV, respectively. The Mn  $2p$  XAS  $L_3$  and  $L_2$  edges (absorption maxima  $\rightarrow$  resonant energies), corresponding to  $2p^6 3d^n \rightarrow 2p^5 3d^{n+1}$  transitions, are found at 640.3 (EX) and 651.4 eV, respectively. The comparison of these values with those reported in literature for a pure metallic thick film of Mn (Ref. 17) shows an almost perfect agreement, proving that the measured film is a true metallic Mn. This conclusion is further supported by the comparison of our XAS spectrum with that of metallic Mn found in literature (inset of Fig. 1).<sup>15,17</sup>

From our data, EB is shifted by about 1.6 eV to lower energy with respect to EX, and comparable shifts have been reported for other transition-metal thick films (V, Cr, Fe).<sup>11</sup> On the contrary, no shift has been found for metallic Ni.<sup>12</sup> It has been proposed that this difference could be ascribed to the different filling of the  $3d$  shells ( $\sim 3d^9$  for Ni,  $d^3$  for V,  $\sim d^4$  for Cr, and  $d^6$  for Fe). The XAS process removes a hole from a correlated  $n$ -hole state ( $n=7,6,4$ ), except for Ni ( $n=1$ , one-particle-like process), and the correlation energy must be supplied by the incoming photon in addition to the BE ( $EX > EB$ ).<sup>11</sup> In our case, Mn metal belongs to the partially filled case ( $d^5$  initial state  $-n=5$ ) and a similar EX-EB shift, scaled according to the  $d$ -band filling, is expected, as observed. In Fig. 1, a shaded area indicates the  $h\nu$  range where the RPE spectra were measured. The photon energy was scanned from 634.0 to 640.9 eV in steps of  $\sim 0.2$  eV, tracking the behavior of the Raman to normal Auger transition along the  $L_3$  edge. The RPES measurements reported in Fig. 2 show the spectra acquired with  $h\nu$  from 636.3 to 649.6 eV. Below 636.3 eV, the shape of the

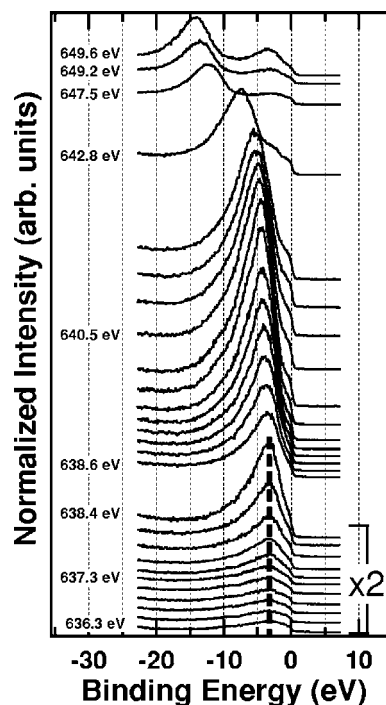


FIG. 2. Valence-band RPE spectra of Mn metal, normalized to flux and number of sweeps. The thick dashed vertical line indicates the Raman-Auger peak at constant BE centered at 3.3 eV below  $E_F$ . Spectra acquired with photon energy  $\leq 638.4$  eV are multiplied by a factor of 2.

valence-band spectra (not reported) is the same as that measured for this particular energy. The spectra are plotted on the BE scale in order to show the Raman-Auger regime below EB. The intensity at 3.3 eV constant BE starts to grow as  $h\nu$  reaches  $\sim 636.5$  eV. This feature shifts following  $h\nu$  and shows a normal Auger (constant KE) behavior for  $h\nu \geq 638.8$  eV. Moreover, its intensity resonates on the  $L_3$  XAS edge. The same conclusions hold, checking the off-resonance-corrected VB spectra (not reported). In Fig. 3, a plot of the  $L_3VV$  Auger KE is presented as a function of  $h\nu$ ,

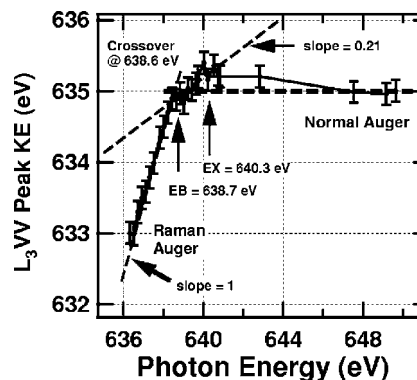


FIG. 3. KE of the Auger  $L_3VV$  peak with respect to the incoming photon energy. The crossover is the energy of the intersection point of the two straight lines fitting the Raman and normal regimes (dashed lines). A dashed line indicates the intermediate mixed Raman to normal regime. Error bars represent the experimental resolution.

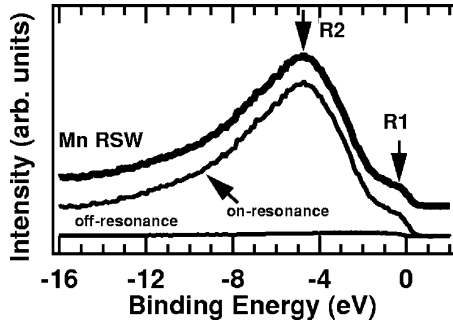


FIG. 4. Mn RSW (thick line) obtained by subtracting the off-resonance spectrum from the resonance one.

and the error bars represent the experimental energy resolution. A linear behavior with slope 1, characteristic of the resonant Raman effect, holds for  $h\nu \leq 638.4$  eV,<sup>12</sup> while for  $h\nu > 647$  eV the KE reaches  $\sim 635.0$  eV (normal Auger regime). There is a broad intermediate energy range where the  $L_3VV$  Auger peak KE value deviates from 635.0 eV: first it is lower for  $h\nu$  between 638.6 and 639.2 eV, then higher for  $h\nu > 639.4$  eV. The crossover energy reported in Fig. 3, and defined in the caption, occurs close to IT as expected and observed in Cr,<sup>11</sup> Ni,<sup>12</sup> and V.<sup>9</sup> Nevertheless, the curve plotted in Fig. 3 is peculiar with respect to other TMs such as Cr and Ni: after following a linear behavior with slope 1 up to the crossover, it deviates following a new linear behavior with slope  $\sim 0.21$  up to  $h\nu = 640.7$  eV (close to EX). After this point, the KE of the  $L_3VV$  Auger peak decreases slightly to reach a constant value of about 635 eV well above EX. It is possible to identify the Raman-Auger onset by integrating the intensity of the VB including the Auger peak with respect to  $h\nu$ . In this way, it is found that the Raman-Auger onset is located at  $\sim 636.5$  eV, and the obtained curve follows the XAS resonant behavior (not shown).

The presence of an energy region between EB and EX where the slope of the curve in Fig. 3 is 0.21 suggests a mixture of Raman and normal Auger behaviors there. A possible explanation could be the persistence of reduced  $3d$  electron localization as  $h\nu$  is increased from EB. Only when  $h\nu \geq EX$  the photoexcited electrons gain enough energy to delocalize faster than the  $2p$  core-hole autoionization time, leaving the system free to deexcite through the normal Auger process.

In order to extract the VB Mn  $3d$ -derived states, following Sangaletti *et al.*,<sup>15</sup> we subtract a nonresonant spectrum ( $h\nu = 634$  eV) from the resonant one collected with  $h\nu = 640.3$  eV and denote it as the resonating spectral weight (RSW). The results are reported in Fig. 4. The clear emission at the Fermi edge (R1) confirms the metallic behavior of the Mn film deposited on the Si substrate. The spectral weight extends well below the Fermi edge, reaching a BE of about 12 eV. This finding supports the presence of strong many-electron effects affecting the final state of the photoemission process.<sup>15</sup> Moreover, the maximum of the RSW is located at about 4.7 eV (R2), together with a shoulder on the high BE side, from  $\sim 6$  to  $\sim 10$  eV. The positions in BE of the two structures R1 and R2 are quite similar to what has been found for the two Mn alloys Mn-doped ZnGeP<sub>2</sub> (Ref. 18) and  $c2 \times 2$  CuMn/Cu(100).<sup>19</sup> Although similar, the main difference is the width of the identified features. In fact, for the metallic Mn we have found larger structures, and this can be explained by a higher degree of delocalization of the Mn  $3d$  electronic states. As a matter of fact, the same conclusion has also been drawn for the metallic surface alloy Mn:Ge(111), which presents a Mn RSW almost identical to our results.<sup>15</sup> In that case, many-electron effects in the final state of the photoemission process were called upon to explain the broadening of the VB Mn-related features.

Being the width of the  $2p_{3/2} \rightarrow 3d$  absorption line  $\sim 3.6$  eV (full width at half maximum) and the energy resolution  $\sim 0.3$  eV, a straightforward analysis of the data in terms of the RRAS technique is feasible.<sup>20</sup> It is then possible to observe the two-hole VB satellite also for Mn, as already demonstrated for Ni, Cr, Fe, and V.<sup>9,11,12</sup> This structure is located at 3.3 eV below  $E_F$  and the crossover from Raman to normal Auger regime is clearly visible and trackable. Another important issue is that the Raman to normal Auger regime crossover is different in the five metals. In Table I, we summarize our findings and compare them to previous studies on  $3d$  TMs. Going from V to Ni, i.e., as the  $d$ -band occupancy and the electronic correlations increase, the difference between EX and EB decreases (first column) while the Raman-Auger peak position relative to  $E_F$  tends to increase (second column). The difference between the photon energy of the Raman-Auger onset and EX varies from the value for V ( $\sim -0.7$  eV) to the values for the other TMs, which are quite similar ( $-3.8$  to  $-5$  eV). The last two col-

TABLE I.  $L_3VV$  Auger decay parameters of  $3d$  transition metals.

	EX-EB	Raman-Auger position relative to $E_F$	Raman-Auger onset relative to EX	EC-EB	Normal Auger onset relative to EX
V <sup>a</sup>	3.0	2.3	-0.7	0	0
Cr <sup>b</sup>	2.0	3.5	$\approx -5$	0	0
Mn <sup>c</sup>	1.6	3.3	$\approx -3.8$	-0.1	$\approx 2$
Fe <sup>b</sup>	0.9	3.2	$\approx -4$	$\approx -1$	0
Ni <sup>d</sup>	0	6.0	$\approx -4$	0	$\approx -0.5$

<sup>a</sup>Reference 9.

<sup>b</sup>Reference 11.

<sup>c</sup>This work.

<sup>d</sup>Reference 12.

umns report the influence of electronic correlations on the transition from Raman to normal Auger behavior, i.e., from a single quantum-mechanical event to a process that can be separated into two steps.<sup>9</sup> The two processes join at EB for the lighter V and Cr without any significant deviation from the two linear behaviors. For the heavier Mn and Fe, there seems to be an intermediate region where both regimes are present (slope < 1), and they both show a mixed Raman to normal Auger behavior in an  $\sim 2$  eV wide region. Ni behaves in a more complex way since it shows deviations from the “two straight line” transition and seems to experience the crossover about 0.5 eV below EB. As reported,<sup>11</sup> the above-mentioned differences in the crossover energy positions may reflect different values for  $U$ , the on-site two-hole repulsion energy, which is closely related to different electronic structures.

The similarity between Mn and Fe, as deduced from the presence of a mixed Raman to normal Auger region, is further evidenced by the comparison of the respective RPES series that look almost identical in terms of shape and evolution. They both show a VB composed of two major features, namely, an emission at the Fermi edge (R1 for Mn) and an asymmetric peak  $\sim 5$  eV from  $E_F$  (R2) that continues to evolve as normal Auger for increasing  $h\nu$ . Differently from V, Cr, and Ni, there are no other resonating structures. From the literature, it is known that Mn and Fe show considerably broader VBs than those of other TMs such as Cr and V, and this has been related to the broadening of their  $MVV$  Auger peaks. This effect has been interpreted as the possible reason for subthreshold ( $3p$  excitation threshold) Auger phenomena, also considering the relatively narrow  $3p$  peaks with respect to the VBs.<sup>21</sup> A similar argument, applied

to the  $LVV$  Auger peaks, can be introduced to explain the present results for Mn and those for Fe.

## CONCLUSIONS

We have measured the resonant photoemission of Mn metal across the  $L_3$  XAS edge tracking the onset of the Raman-Augur regime and its transition to a normal Auger regime. Above the ionization threshold, the pure Raman-Augur turns into a mixed Raman to normal Auger regime. This suggests the coexistence of weakly localized and delocalized Mn  $3d$  electronic states up to the resonance energy (EX). Only when  $h\nu$  is high enough the system evolves into a true normal Auger regime (photoelectrons delocalize or escape to vacuum). Moreover, Mn metal shows a transition from Raman to normal Auger regime that is different from other TMs, probably because of their different electronic structures. The RRAS, nevertheless, demonstrates the capability to detect the two-hole VB satellite in Mn, showing it at 3.3 eV below  $E_F$ . Using the same RPES data, we have also extracted the Mn partial density of states finding an evident Fermi edge and a spectral weight extending well below ( $\sim 12$  eV)  $E_F$  due to many-electron effects in the PE final state. The width of these structures suggests a delocalization of the Mn  $3d$  electronic states. This conclusion, obtained from the on-resonance (EX) spectrum, is in agreement with the above-mentioned results reporting a delocalized character for  $h\nu \geq EX$ .

## ACKNOWLEDGMENT

The authors would like to thank Bryan Doyle for proof-reading the manuscript.

- 
- <sup>1</sup>M. Wuttig, T. Flores, and C. C. Knight, Phys. Rev. B **48**, 12082 (1993).
- <sup>2</sup>S. Lee, R. Rousseau, and C. Wells, Phys. Rev. B **46**, 12121 (1992).
- <sup>3</sup>D. E. Eastman, J. Appl. Phys. **40**, 1387 (1969).
- <sup>4</sup>L. Ley, O. B. Dabbousi, S. P. Kowalczyk, F. R. McFeely, and D. A. Shirley, Phys. Rev. B **16**, 5372 (1977).
- <sup>5</sup>C.-O. Almbladh and L. Hedin, in *Handbook on Synchrotron Radiation*, edited by E. E. Koch (North-Holland, Amsterdam, 1983), Vol. 1, and references therein.
- <sup>6</sup>J. W. Allen, in *Synchrotron Radiation Research*, edited by R. Z. Bachrach (Plenum, New York, 1992), Vol. 25.
- <sup>7</sup>L. Sangaletti, S. Pagliara, F. Parmigiani, A. Goldoni, L. Floreano, A. Morgante, and V. Aguekian, Phys. Rev. B **67**, 233201 (2003).
- <sup>8</sup>M. C. Richter, P. Bencok, R. Brochier, V. Ilakovac, O. Heckmann, G. Paolucci, A. Goldoni, R. Larciprete, J.-J. Gallet, F. Chevrier, G. Van der Laan, and K. Hricovini, Phys. Rev. B **63**, 205416 (2001).
- <sup>9</sup>V. Ilakovac, M. Kralj, P. Pervan, M. C. Richter, A. Goldoni, R. Larciprete, L. Petaccia, and K. Hricovini, Phys. Rev. B **71**, 085413 (2005).
- <sup>10</sup>T. Kaurila, R. Uhrberg, and J. Väyrynen, J. Electron Spectrosc. Relat. Phenom. **88-91**, 399 (1998).
- <sup>11</sup>S. Hüfner, S.-H. Yang, B. S. Mun, C. S. Fadley, J. Schäfer, E. Rotenberg, and S. D. Kevan, Phys. Rev. B **61**, 12582 (2000).
- <sup>12</sup>M. Weinelt, A. Nilsson, M. Magnuson, T. Wiell, N. Wassdahl, O. Karis, A. Föhlich, N. Mårtensson, J. Stöhr, and M. Samant, Phys. Rev. Lett. **78**, 967 (1997).
- <sup>13</sup>S. Raaen and V. Murgai, Phys. Rev. B **36**, 887 (1987).
- <sup>14</sup>O. Rader, C. Pampuch, A. M. Shikin, W. Gudat, J. Okabayashi, T. Mizokawa, A. Fujimori, T. Hayashi, M. Tanaka, A. Tanaka, and A. Kimura, Phys. Rev. B **69**, 075202 (2004).
- <sup>15</sup>L. Sangaletti, D. Ghidoni, S. Pagliara, A. Goldoni, A. Morgante, L. Floreano, A. Cossaro, M. C. Mozzati, and C. B. Azzoni, Phys. Rev. B **72**, 035434 (2005).
- <sup>16</sup>M. Zangrando, M. Finazzi, G. Paolucci, G. Comelli, B. Diviacco, R. P. Walker, D. Cocco, and F. Parmigiani, Rev. Sci. Instrum. **72**, 1313 (2001).
- <sup>17</sup>J. Fink, Th. Müller-Heinzerling, B. Scheerer, W. Speier, F. U. Hillebrecht, J. C. Fuggle, J. Zaanen, and G. A. Sawatzky, Phys. Rev. B **32**, 4899 (1985).
- <sup>18</sup>Y. Ishida, D. D. Sarma, K. Okazaki, J. Okabayashi, J. I. Hwang, H. Ott, A. Fujimori, G. A. Medvedkin, T. Ishibashi, and K. Sato, Phys. Rev. Lett. **91**, 107202 (2003).
- <sup>19</sup>O. Rader, W. Gudat, C. Carbone, E. Vescovo, S. Blügel, R. Kläsges, W. Eberhardt, M. Wuttig, J. Redinger, and F. J. Himpsel, Phys. Rev. B **55**, 5404 (1997).
- <sup>20</sup>G. B. Armen and H. Wang, Phys. Rev. A **51**, 1241 (1995).
- <sup>21</sup>T. Kaurila, J. Väyrynen, and M. Isokallio, J. Phys.: Condens. Matter **9**, 6533 (1997).